Published in final edited form as:
Dev Cell. 2011 March 15; 20(3): 397–404. doi:10.1016/j.devcel.2011.01.010.

Retinoic acid production by endocardium and epicardium is an injury response essential for zebrafish heart regeneration

Kazu Kikuchi[1], **Jennifer E. Holdway**[1], **Robert J. Major**[1,4], **Nicola Blum**[2], **Randall D. Dahn**[3], **Gerrit Begemann**[2], and **Kenneth D. Poss**[1,3,*]

[1]Department of Cell Biology and Howard Hughes Medical Institute, Duke University Medical Center, Durham, North Carolina 27710, USA.

[2]Lehrstuhl für Zoologie und Evolutionsbiologie, Department of Biology, University of Konstanz, D-78457 Konstanz, Germany.

[3]Mount Desert Island Biological Laboratory, Salisbury Cove, Maine 04672, USA.

SUMMARY

Zebrafish heart regeneration occurs through the activation of cardiomyocyte proliferation in areas of trauma. Here, we show that within three hours of ventricular injury, the entire endocardium undergoes morphological changes and induces expression of the retinoic acid (RA)-synthesizing enzyme *raldh2*. By one day post-trauma, *raldh2* expression becomes localized to endocardial cells at the injury site, an area that is supplemented with *raldh2*-expressing epicardial cells as cardiogenesis begins. Induced transgenic inhibition of RA receptors or expression of an RA-degrading enzyme blocked regenerative cardiomyocyte proliferation. Injured hearts of the ancient fish *Polypterus senegalus* also induced and maintained robust endocardial and epicardial *raldh2* expression coincident with cardiomyocyte proliferation, while poorly regenerative infarcted murine hearts did not. Our findings reveal that the endocardium is a dynamic, injury-responsive source of RA in zebrafish, and indicate key roles for endocardial and epicardial cells in targeting RA synthesis to damaged heart tissue and promoting cardiomyocyte proliferation.

INTRODUCTION

Studies of non-mammalian vertebrates that naturally regenerate damaged cardiac muscle stand to guide mammalian heart regeneration. After resection of up to 20% of their single cardiac ventricle, zebrafish replace lost muscle with minimal scar formation (Poss et al., 2002). Genetic lineage-tracing studies recently showed that existing cardiomyocytes (CMs), as opposed to a reserve population of undifferentiated progenitor cells, are the major source of regenerated muscle (Jopling et al., 2010; Kikuchi et al., 2010). Little is currently known about cellular and molecular influences on proliferation of these source CMs.

*Correspondence: kenneth.poss@duke.edu.
[4]Present address: Department of Biology, Indiana University of Pennsylvania, Indiana, Pennsylvania 15701, USA.

SUPPLEMENTAL INFORMATION

Supplemental Information includes Supplemental Experimental Procedures and three figures.

Recent studies have implicated the epicardium, a mesothelial layer surrounding the cardiac chambers, in promoting heart regeneration. This structure acts as progenitor tissue for fibroblasts, vascular support cells, and possibly CMs, during embryonic heart development, when evidence also supports its role as a paracrine effector of myocardial growth (Gittenberger-de Groot et al., 2010). Within 1–2 days of injury to the adult zebrafish heart, virtually all epicardial tissue covering both chambers is activated to induce embryonic markers and proliferate. Epicardial cells accumulate in the wound site by 7–14 days post-amputation (dpa), where their recruitment in an Fgf- and Pdgf-dependent manner is required for continued muscle regeneration (Kim et al., 2010; Lepilina et al., 2006).

A conspicuous marker of epicardial cells that participate in regeneration is *raldh2*, an enzyme responsible for synthesis of the morphogenetic factor retinoic acid (RA) (Lepilina et al., 2006). RA is converted from Vitamin A via a two-step metabolic pathway, and transduces signals by binding to heterodimers formed between nuclear hormone receptors. RA removal occurs through conversion into more polar metabolites by a family of cytochrome P450 (Cyp) enzymes. RA signaling is essential for normal cardiac development during embryogenesis, where it has both early patterning roles and later mitogenic roles (Hoover et al., 2008; Kastner et al., 1994; Ryckebusch et al., 2008; Sucov et al., 1994; Waxman et al., 2008). While epicardial *raldh2* expression is suggestive, the extent and functions of RA synthesis and signaling during heart regeneration have not been determined.

Here, we assessed the behavior and potential functions during regeneration of the endocardium, an endothelial cell layer that lines cardiac muscle and separates it from ventricular and atrial lumens. Endocardial cells play a critical role in growth and maturation of the embryonic heart, through interaction with CMs and production of growth factors (Smith and Bader, 2007). We find that the endocardium is an unsuspected, dynamic source of RA during adult heart regeneration, and that RA signaling is critical for injury-induced CM proliferation. We also show that RA production by epicardial and endocardial cells is a response subdued in mouse but shared by evolutionarily distant species capable of cardiac regeneration, establishing a molecular mechanism by which endocardial and epicardial cells help initiate heart regeneration.

RESULTS

Morphological and Molecular Changes in Endocardium during Heart Regeneration

To examine morphological changes in the endocardium, we used transmission electron microscopy (TEM) to assess ventricles at 1 hour post-amputation (hpa), 3 hpa, 1 dpa, 3 dpa, and 7 dpa. Endocardial cells in uninjured ventricles typically possess elongated nuclei and thin cell bodies that adhere tightly to underlying myofibers (Figure 1A). When visualized in injured ventricles at 3 hpa, and typically as early as 1 hpa, endocardial cells often appeared rounded and showed detachment from the underlying myofibers, likely reflecting increased permeability (Figure 1B). These morphological changes were detected in the ventricle in areas both near to and distant from the injured apex. We next looked for morphological differences during regeneration between endocardial cells at the injury site and those away from the wound. Using TEM, we found that endocardial tissue distant from the injury typically appeared grossly normal by 1 and 3 dpa (Figure 1C). By contrast, endocardium at the injury site retained a rounded, disorganized appearance through at least 7 dpa, a timepoint of robust early CM proliferation (Poss et al., 2002) (Figure 1D). Thus, dynamic, morphological changes occur in endocardial tissue after cardiac injury that initially affect most ventricular endocardial cells, but appear to localize to the injury site during regeneration.

To determine molecular profiles that might correspond to these ultrastructural changes, we examined several molecular markers. We identified two developmental markers that are rapidly induced in the endocardium following injury: the RA-synthesizing enzyme *raldh2*, and the transmembrane receptor *heart of glass* (*heg*) (Mably et al., 2003). These genes were induced strongly in endocardial cells throughout both chambers by 3 hpa (Figure 1E, F, H and Figure S1A, B), with expression more commonly detectable at 1 hpa only in atrial endocardium (Figure S1C). By 6 hpa, *raldh2* remained strongly induced throughout both chambers, while *heg* expression was diminished (Figure 1G and data not shown). Remarkably, as early as 24 hours after injury, robust endocardial *raldh2* induction became localized exclusively to the ventricular injury site, where it could be detected throughout the initial stages of myocardial regeneration (7–14 days; Figure 1I). *raldh2* was not comparably induced in endothelial cells of the aorta or coronary vessels at 6 hpa or 3 dpa (data not shown), suggesting that the injury response is focused to endocardial endothelium. By 7 dpa, the injury site also contains *raldh2*-expressing epicardial cells that surround the fibrin clot (Figure 1J, K) (Lepilina et al., 2006). Thus, endocardial *raldh2* induction occurred in a similar spatiotemporal pattern as the ultrastructural changes we detected, representing an early injury response involving most or all endocardial cells before focusing to the injury site.

To further characterize endocardial changes associated with regeneration, we generated transgenic strains reporting fluorescent protein expression from different cardiovascular transcription factor gene loci (*flk1:DsRed2*, *hand2:EGFP*, *gata5:EGFP*). Analysis of 7 dpa samples using these and other reagents showed enhanced expression of Raldh2 protein and vascular endothelial markers *fli1* and *flk1* in endocardial cells adjacent to regenerating myocardium (Figure 1K–O). The transcription factors *hand2* and *gata5*, both required for generation of the earliest CMs in zebrafish embryos (Reiter et al., 1999; Yelon et al., 2000), were also expressed at higher levels within injury site endocardium (Figure 1P, Q). Consistent with our TEM observations, we observed rounded and detached morphology in endocardial cells enriched with these markers at 7 dpa by confocal microscopy (Figure 1L–Q). These results indicate that endocardium adjacent to regenerating muscle sustains a distinct morphology and expression profile, underscored by increases in RA synthesis and expression of cardiovascular transcription factors.

raldh2 is Induced in Response to Diverse Cardiac Injuries

We performed several experiments to determine the nature of the signals that activate or maintain this regenerative endocardial profile. The endocardium showed little or no *raldh2* induction after sham injury (opening the pericardial sac) or pericardial saline-injection (data not shown), procedures that activate *raldh2* expression in epicardial cells (Wills et al., 2008). However, a penetrating wound with a glass needle robustly induced endocardial *raldh2* expression and morphological changes detectable by confocal microscopy. *raldh2* induction was first organ-wide (data not shown) and then focused to the stab injury, indicating that tissue removal is not required for endocardial activation (Figure 3A–C). Next, we examined whether inflammatory stress activated the endocardium in the absence of mechanical injury. Lipopolysaccharide (LPS) causes systemic inflammation and increased permeability of endothelial cells when injected in animals. When injected intraperitoneally into uninjured wild-type fish, LPS induced robust, organ-wide *raldh2* expression in the endocardium within one day (Figure 3D–H). Finally, to test whether a systemic factor maintains the activated endocardium, we removed hearts from adult zebrafish and cultured them *in vitro* for 7 days. These hearts contract for many days under these conditions, although they will form spontaneous internal infarcts. Strikingly, *raldh2*, *hand2*, and *gata5* were each enriched in endocardial cells lining such infarcts (Figure 3I–L). In total, these

results indicate that endocardial RA synthesis is a fundamental response to cardiac injury and inflammation, and that it is maintained at sites of injury via local interactions.

RA Signaling is Required for Cardiomyocyte Proliferation during Zebrafish Heart Regeneration

To test whether RA signaling is required for regeneration of adult CMs, we first examined expression of Retinoid acid receptors (RARs) and Retinoid X receptors (RXRs) during heart regeneration. We detected expression of several receptors by RT-PCR in endothelial/endocardial and CM populations dissociated and sorted from uninjured and 7 dpa *cmlc2:EGFP*; *flk1:DsRed2* ventricles using flow cytometry (Figure S2A, B).

To determine the requirement for signaling through these expressed receptors, we generated a transgenic strain that facilitates inducible expression of a dominant-negative zebrafish *RAR-alpha* (*hsp70:dn-zrar*) throughout all tissues of the animal. A single 37°C heat-shock to 24-hour post-fertilization (hpf) embryos caused developmental defects by 72 hpf characteristic of impaired retinoid signaling, including cardiac dysmorphology and the reduction or absence of pectoral fins (Figure S3A–D). To test effects on cardiac regeneration, we heat-shocked adult transgenic and wild-type clutchmates once at 6 dpa, and collected ventricles one day later. This treatment maintained *dn-zrar* at highest levels in CMs, and weakly in other cardiac cell types, for >24 hours (Figure S3E, F). We found that *hsp70:dn-zrar* ventricles had an 86% lower CM proliferation index than wild-type ventricles (Figure 3A, B). Similar inhibitory effects on CM proliferation were obtained with a second line of *hsp70:dn-zrar* animals (Figure SG). Apoptotic CMs are rare in uninjured ventricles, commonly observed in the injury site at 2 dpa, and less frequent at 7 dpa. Quantification of TUNEL staining after induced RAR inhibition indicated these same dynamics with no significant differences from wild-types (Figure S3H, I). We also observed no significant effects of *dn-zrar* induction on CM proliferation during animal growth stimulated by low aquarium density, a treatment that moderately increases endocardial *raldh2* expression throughout the ventricle and atrium (Wills et al., 2008) (data not shown). This specificity suggests that RA signaling has a more prominent or dedicated role in injury-induced CM proliferation than in low density-stimulated cardiac growth.

We performed similar experiments with a different transgenic strain (*hsp70:cyp26a1*), in which heat-shock treatment induces expression of an RA-degrading Cyp26 enzyme. In the same heat-shock regimen, we found that the CM proliferation index in *hsp70:cyp26a1* ventricles was decreased by 87% from that of clutchmates, similar to the levels in *hsp70:dn-zrar* ventricles (Figure 3C, D). Epicardial proliferation appeared similar under the heat-shock treatment in both strains, indicating no gross effects of *dn-zrar* or *cyp26a1* expression on this cell population (Figure 3A, C). We also examined whether exogenous RA, or TTNPB, a synthetic retinoid agonist reported to stimulate RARs in Xenopus embryos (Shiotsugu et al., 2004), was sufficient to induce CM proliferation. Agonist treatment had no detectable effects on endocardial Raldh2 expression or gross morphology (data not shown), nor did it have significant effects on CM proliferation in any of several treatment regimens (data not shown). This suggests that RA produced by endocardial and epicardial Raldh2 is a permissive, rather than instructive, signal for regeneration.

Evolutionarily Shared Response of RA Synthesis during Heart Regeneration

To determine whether this cellular and molecular response to *in situ* myocardial loss is present in other non-mammalian species with potentially high regenerative capacity, we performed partial ventricular resection surgeries in *Polypterus senegalus*. Polypterus represent the most basally branching member of extant ray-finned fishes (Actinopterygii), with the last common ancestor with other actinopterygian fishes like teleosts having lived

~400 million years ago (Inoue et al., 2003). Young polypteri displayed CM proliferation at injury sites by 7 days after a resection or stab wound, indicative of a regenerative response (Figure 4E–G). Similar to zebrafish, *raldh2* expression was undetectable in the uninjured ventricle, but induced in endocardial cells near and away from the injury site by 6 hpa. We did not see a full ventricle-wide induction of endocardial *raldh2*; however, epicardial cells did induce *raldh2* in a ventricle-wide manner. As in zebrafish, *raldh2* expression was maintained at 7 dpa in endocardial and epicardial cells in regions of injury and CM proliferation (Figure 4A–D, H).

To determine whether a similar response is present in the poorly regenerative mammalian heart, we performed coronary artery ligation in mice and assessed infarcted ventricles for *Raldh2* expression. We did not detect expression in the uninjured left ventricle or at 6 hours post-ligation (hpl), but observed *Raldh2*-positive cells within the lesions that resembled fibroblasts and/or inflammatory cells by 1 day post-ligation (dpl) (Figure 4I, J). More of these cells accumulated by 3 dpl (Figure 4K), but numbers were greatly reduced by 7 dpl (Figure 4L). By this timepoint, *Raldh2*-positive epicardial tissue was occasionally observed near the wound (Figure 4L). However, we detected no endocardial *Raldh2* expression near or distant from the trauma at any timepoint that we tested (6 hpl, or 1, 3, 7, and 14 dpl) (Figure 4I–L and data not shown), distinguishing mice in this respect from species with higher cardiac regenerative capacity.

DISCUSSION

We propose that dynamic and sustained RA production by the zebrafish endocardium, in addition to the epicardium, is an important component of the capacity to achieve local regenerative cardiogenesis. Indeed, we show it is a feature of a second non-mammalian vertebrate that we find also to be capable of injury-induced CM proliferation, *Polypterus senegalus*. The non-regenerative mouse heart does increase RA synthesis in response to injury; however, the cell types, prominence, and kinetics of RA production in response to myocardial damage are quite different (Figure 4M). These differences implicate the endocardium and non-myocardial RA production as targets in attempts to increase regenerative capacity in the injured mammalian heart.

The molecular mechanisms by which the endocardium is activated and induces *raldh2* will require further clarification. Clues may come from the fact that we could stimulate *raldh2* induction by LPS injection, and that injury triggered organ-wide morphologic changes in the endocardium. One possibility is that growth factors or cytokines are released after injury and impact the permeability of endocardial cells (Nagy et al., 2008), with *raldh2* induction being a response to this change. Indeed, Heg is required for vascular permeability in mice (Kleaveland et al., 2009), and *heg* is shown here to be a robust early marker of the activated endocardium in zebrafish. To date, we have not been able to induce a strong, organ-wide response by injection of individual murine pro-inflammatory factors such as IL-6, IL-1β, IFNγ, and TNFαK.K. and K.D.P., unpublished results).

It has been known for several years that RA signaling is critical for myocardial proliferation during embryonic heart development. While it was initially suspected that embryonic ventricular compact CMs receive epicardial RA and are instructed to proliferate, a number of experiments argue against this mechanism. These include the fact that RXRα function was not required in CMs for normal ventricular cardiogenesis (Chen et al., 1998; Merki et al., 2005; Subbarayan et al., 2000; Tran and Sucov, 1998), and that RA was insufficient on its own as a mitogen in cultured cardiac slices (Stuckmann et al., 2003). Our findings appear to parallel these studies, given that RA presence and reception were required for regenerative proliferation, yet we could not influence CM proliferation by introducing RAR

ligand. It is also possible that RA production within or distant from areas of injury has multiple functions germane to different cardiac cell types and heart regeneration, a relevant issue during embryonic cardiac growth (Brade et al., 2011; Jenkins et al., 2005). As mechanisms by which RA influences cardiac proliferation and patterning in embryos are uncovered, these findings are likely to provide insight into the influences of endocardial and epicardial RA during heart regeneration.

EXPERIMENTAL PROCEDURES

Fish and Injury Models

Outbred Ekkwill strain (EK) or EK/AB mixed background zebrafish 6–12 months of age were used for ventricular resection surgeries as described previously (Poss et al., 2002). Similarly, ventricular resection surgeries were performed on juvenile *Polypterus senegalus* (~4 inches in length). Pulled glass needles of ~50 μm in diameter and irridectomy scissors were used for stab injuries of zebrafish and polypterus ventricles, respectively. All transgenic strains were analyzed as hemizygotes, and details of their construction are described in Supplemental Methods. For heat-shock experiments, *hsp70:dn-zrar*, *hsp70:cyp26a1*, and control clutchmates were given a single heat-shock at 37 or 38°C at 6 dpa using conditions described previously (Wills et al., 2008). Fish were transferred to a standard aquarium at 26°C after the heat-shock, and hearts were collected at 7 dpa for proliferation analyses. LPS (Escherichia coli Serotype 011:B4) (Sigma-Aldrich) was dissolved in PBS at 2.5 mg/ml, and ~10 μl of the LPS solution was intraperitoneally injected into adult zebrafish. For experiments with mice, infarcts were induced by ligation of the left anterior descending artery in C57BL/6 mice at 8–10 weeks of age, as described elsewhere (Curcio et al., 2006). Infarcted hearts were transversely sectioned, and images of the left ventricular wall were shown.

Histological Methods

Zebrafish and polypterus hearts were dissected and fixed in 4% paraformaldehyde (PFA) at room temperature for 1 hour. All histological analyses were performed using 10 μm cryosections. *In situ* hybridization was performed using digoxigenin-labeled cRNA probes as described previously (Poss et al., 2002). Primary and secondary antibody staining was performed as previously described (Lepilina et al., 2006), except for Mef2 and PCNA double staining, in which an heat-induced antigen retrieval using citrate buffer was performed. TUNEL assays were performed as described (Wills et al., 2008), The number of manually counted $TUNEL^+$ events and the area of muscle sampled (mm^2) were totaled from 3 ventricular sections showing large injuries (except in uninjured animals), from each animal. Antibodies are described in Supplemental Methods.

In situ hybridization and immunofluorescence images were taken using a Leica DM6000 microscope with a Retiga-EXi camera (Q-IMAGING). Confocal images were taken using a Leica SP2 or SP5 confocal microscope. For images of *in situ* hybridization experiments, autofluorescence of muscle in the red channel was overlaid to aid visualization of signals. To quantify CM proliferation, 3 sections showing the largest wounds were selected from each heart, and images were taken using a 20X objective. The number of $Mef2^+$ and $Mef2^+PCNA^+$ cells were manually counted within a defined region typically including almost all $Mef2^+PCNA^+$ CMs near the injury (216 pixels in vertical). The percentages of $Mef2^+PCNA^+$ cells from the 3 selected sections were averaged to determine a proliferation index for each heart.

For TEM, injured hearts were fixed in 2% glutaraldehyde/4% formaldehyde. Tissue was embedded using the EMbed 812 resin kit (with DMP-30) (EMS) and sectioned to 70–90 nm

thickness using Ultracut or Ultracut E ultra-microtomes (Leica). Microscopy was performed on a FEI Tecnai G2 Twin (200kv) transmission electron microscope and images were obtained using a FEI Eagle camera.

Heart Explant Culture

Hearts were extracted and rinsed with Liebovit's L-15 medium (plus L-glutamine, minus phenol red), supplemented with 10% FCS, 1% Penicillin, Streptomycin, Fungizone (GIBCO). A single heart was transferred to a single well of a six- or twelve-well plate containing this medium, and samples were cultured for 7 days, with medium changes every 2 days.

Supplementary Material

Refer to Web version on PubMed Central for supplementary material.

Acknowledgments

We thank H. Rockman and L. Mao for performing murine coronary ligation injuries and tissue collection, J. Burris, A. Eastes, and P. Williams for zebrafish care, M. Gignac for help with electron microscopy, X. Meng and Abmart for the Raldh2 antibody, H. Kasai for help with cell sorting, M. Bagnat, F. Conlon, and lab members for comments on the manuscript, and J. Mably, S. Jin, G. Felsenfeld, A. Nechiporuk, for plasmids. K.K. was supported by postdoctoral fellowships from AHA and JSPS. R.J.M. was supported by NIH training grant 2 T-32 HL007101-31. This work was supported by grants from NHLBI, AHA, Pew Charitable Trusts, and Salisbury Cove Research Fund to K.D.P.

REFERENCES

Brade T, Kumar S, Cunningham TJ, Chatzi C, Zhao X, Cavallero S, Li P, Sucov HM, Ruiz-Lozano P, Duester G. Retinoic acid stimulates myocardial expansion by induction of hepatic erythropoietin which activates epicardial Igf2. Development (Cambridge, England). 2011; 138:139–148.

Chen J, Kubalak SW, Chien KR. Ventricular muscle-restricted targeting of the RXRalpha gene reveals a non-cell-autonomous requirement in cardiac chamber morphogenesis. Development (Cambridge, England). 1998; 125:1943–1949.

Curcio A, Noma T, Naga Prasad SV, Wolf MJ, Lemaire A, Perrino C, Mao L, Rockman HA. Competitive displacement of phosphoinositide 3-kinase from beta-adrenergic receptor kinase-1 improves postinfarction adverse myocardial remodeling. American journal of physiology. 2006; 291:H1754–H1760. [PubMed: 16699071]

Gittenberger-de Groot AC, Winter EM, Poelmann RE. Epicardium-derived cells (EPDCs) in development, cardiac disease and repair of ischemia. J Cell Mol Med. 2010; 14:1056–1060. [PubMed: 20646126]

Hoover LL, Burton EG, Brooks BA, Kubalak SW. The expanding role for retinoid signaling in heart development. The Scientific World Journal. 2008; 8:194–211.

Inoue JG, Miya M, Tsukamoto K, Nishida M. Basal actinopterygian relationships: a mitogenomic perspective on the phylogeny of the "ancient fish". Mol Phylogenet Evol. 2003; 26:110–120. [PubMed: 12470943]

Jenkins SJ, Hutson DR, Kubalak SW. Analysis of the proepicardium-epicardium transition during the malformation of the RXRalpha−/− epicardium. Dev Dyn. 2005; 233:1091–1101. [PubMed: 15861408]

Jopling C, Sleep E, Raya M, Marti M, Raya A, Belmonte JC. Zebrafish heart regeneration occurs by cardiomyocyte dedifferentiation and proliferation. Nature. 2010; 464:606–609. [PubMed: 20336145]

Kastner P, Grondona JM, Mark M, Gansmuller A, LeMeur M, Decimo D, Vonesch JL, Dolle P, Chambon P. Genetic analysis of RXR alpha developmental function: convergence of RXR and RAR signaling pathways in heart and eye morphogenesis. Cell. 1994; 78:987–1003. [PubMed: 7923367]

Kikuchi K, Holdway JE, Werdich AA, Anderson RM, Fang Y, Egnaczyk GF, Evans T, Macrae CA, Stainier DY, Poss KD. Primary contribution to zebrafish heart regeneration by gata4(+) cardiomyocytes. Nature. 2010; 464:601–605. [PubMed: 20336144]

Kim J, Wu Q, Zhang Y, Wiens KM, Huang Y, Rubin N, Shimada H, Handin RI, Chao MY, Tuan TL, et al. PDGF signaling is required for epicardial function and blood vessel formation in regenerating zebrafish hearts. Proceedings of the National Academy of Sciences of the United States of America. 2010; 107:17206–17210. [PubMed: 20858732]

Kleaveland B, Zheng X, Liu JJ, Blum Y, Tung JJ, Zou Z, Sweeney SM, Chen M, Guo L, Lu MM, et al. Regulation of cardiovascular development and integrity by the heart of glass-cerebral cavernous malformation protein pathway. Nature medicine. 2009; 15:169–176.

Lepilina A, Coon AN, Kikuchi K, Holdway JE, Roberts RW, Burns CG, Poss KD. A dynamic epicardial injury response supports progenitor cell activity during zebrafish heart regeneration. Cell. 2006; 127:607–619. [PubMed: 17081981]

Mably JD, Mohideen MA, Burns CG, Chen JN, Fishman MC. Heart of glass regulates the concentric growth of the heart in zebrafish. Curr Biol. 2003; 13:2138–2147. [PubMed: 14680629]

Merki E, Zamora M, Raya A, Kawakami Y, Wang J, Zhang X, Burch J, Kubalak SW, Kaliman P, Belmonte JC, et al. Epicardial retinoid X receptor alpha is required for myocardial growth and coronary artery formation. Proceedings of the National Academy of Sciences of the United States of America. 2005; 102:18455–18460. [PubMed: 16352730]

Nagy JA, Benjamin L, Zeng H, Dvorak AM, Dvorak HF. Vascular permeability, vascular hyperpermeability and angiogenesis. Angiogenesis. 2008; 11:109–119. [PubMed: 18293091]

Poss KD, Wilson LG, Keating MT. Heart regeneration in zebrafish. Science (New York, NY). 2002; 298:2188–2190.

Reiter JF, Alexander J, Rodaway A, Yelon D, Patient R, Holder N, Stainier DY. Gata5 is required for the development of the heart and endoderm in zebrafish. Genes & development. 1999; 13:2983–2995. [PubMed: 10580005]

Ryckebusch L, Wang Z, Bertrand N, Lin SC, Chi X, Schwartz R, Zaffran S, Niederreither K. Retinoic acid deficiency alters second heart field formation. Proceedings of the National Academy of Sciences of the United States of America. 2008; 105:2913–2918. [PubMed: 18287057]

Shiotsugu J, Katsuyama Y, Arima K, Baxter A, Koide T, Song J, Chandraratna RA, Blumberg B. Multiple points of interaction between retinoic acid and FGF signaling during embryonic axis formation. Development (Cambridge, England). 2004; 131:2653–2667.

Smith TK, Bader DM. Signals from both sides: Control of cardiac development by the endocardium and epicardium. Semin Cell Dev Biol. 2007; 18:84–89. [PubMed: 17267246]

Stuckmann I, Evans S, Lassar AB. Erythropoietin and retinoic acid, secreted from the epicardium, are required for cardiac myocyte proliferation. Developmental biology. 2003; 255:334–349. [PubMed: 12648494]

Subbarayan V, Mark M, Messadeq N, Rustin P, Chambon P, Kastner P. RXRalpha overexpression in cardiomyocytes causes dilated cardiomyopathy but fails to rescue myocardial hypoplasia in RXRalpha-null fetuses. The Journal of clinical investigation. 2000; 105:387–394. [PubMed: 10675365]

Sucov HM, Dyson E, Gumeringer CL, Price J, Chien KR, Evans RM. RXR alpha mutant mice establish a genetic basis for vitamin A signaling in heart morphogenesis. Genes & development. 1994; 8:1007–1018. [PubMed: 7926783]

Tran CM, Sucov HM. The RXRalpha gene functions in a non-cell-autonomous manner during mouse cardiac morphogenesis. Development (Cambridge, England). 1998; 125:1951–1956.

Waxman JS, Keegan BR, Roberts RW, Poss KD, Yelon D. Hoxb5b acts downstream of retinoic acid signaling in the forelimb field to restrict heart field potential in zebrafish. Developmental cell. 2008; 15:923–934. [PubMed: 19081079]

Wills AA, Holdway JE, Major RJ, Poss KD. Regulated addition of new myocardial and epicardial cells fosters homeostatic cardiac growth and maintenance in adult zebrafish. Development (Cambridge, England). 2008; 135:183–192.

Yelon D, Ticho B, Halpern ME, Ruvinsky I, Ho RK, Silver LM, Stainier DY. The bHLH transcription factor hand2 plays parallel roles in zebrafish heart and pectoral fin development. Development (Cambridge, England). 2000; 127:2573–2582.

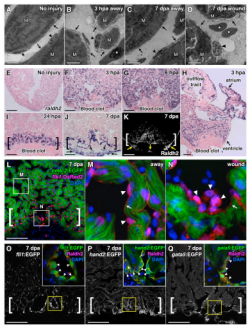

Figure 1. Resection of the Ventricular Apex Stimulates Immediate, Organ-wide Morphological and Molecular Changes in Endocardium

(A–D) Transmission electron microscope (TEM) analyses of endocardium in uninjured (A) and injured ventricles (B–D). Arrowheads, endocardial nuclei. Arrows, endocardial cell bodies. M, cardiac muscle. Asterisk, red blood cell. Scale bar, 2 μm.

(E–K) *raldh2* expression assessed by *in situ* hybridization (E–J) and Raldh2 immunostaining (K) in uninjured (E) and injured (F–K) ventricles. Brackets in (I–K), injury site. Arrows in (J, K), epicardial cells. Scale bar (E–Q), 100 μm.

(L–N) Confocal images of altered endocardial cell shape, and enhanced *flk1* driven DsRed2 fluorescence in the injury site (A, brackets) in a 7 dpa *cmlc2:EGFP; flk1:DsRed2* double transgenic ventricle. Arrowheads, endocardial nuclei. Arrows, endocardial lining of myofiber. An antibody against DsRed was used. DAPI (4'-6-Diamidino-2-phenylindole) stains nuclei.

(O–Q) Sections of 7 dpa *fli1:EGFP* (O), *hand2:EGFP* (P), or *gata5:EGFP* (Q) transgenic ventricles. Brackets, injury sites. Arrowheads in inset, $Raldh2^{+}/EGFP^{+}$ endocardial nuclei with rounded morphology (G–I).

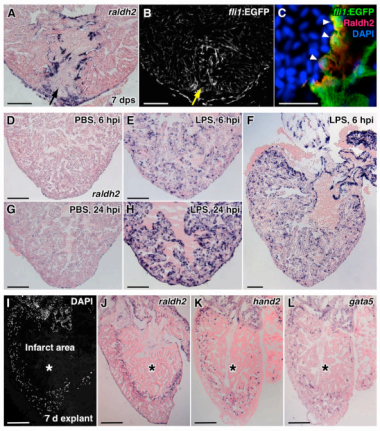

Figure 2. Induction of *raldh2* Expression in Various Injury Models

(A,B) Stab injuries into the ventricular apex assessed for *raldh2* induction (A) and *fli1*:EGFP expression (B) at 7 days post-stab (dps). Arrows, needle entry site. Scale bar, 100 μm.

(C) Confocal image of Raldh2 immunofluorescence in *fli1*:EGFP^{+} endocardial cells with rounded morphology at the injury site (arrowheads). Scale bar, 20 μm.

(D–H) *raldh2* induction after intraperitoneal LPS or vehicle (PBS) injection. Scale bar, 100 μm (D–L).

(I–L) Endocardial *raldh2* (J), *hand2* (K), and *gata5* (L) expression surrounding spontaneous infarcts (asterisks) within cultured ventricular explants. Dead cardiac tissue was identifiable by the absence of cell nuclei (I).

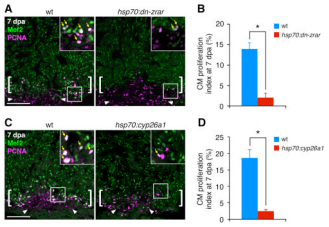

Figure 3. Transgenic Inhibition of RA Signaling Blocks Cardiomyocyte Proliferation during Regeneration

(A) Assessment of $Mef2^{+}PCNA^{+}$ cells (arrows) in wild-type (wt) and *hsp70:dn-zrar* transgenic fish at 7 dpa, after a single heat-shock at 6 dpa. Maximum projection images of 10 μm z-stacks are shown. Insets, high-magnification images of the rectangle. Arrowheads, proliferating epicardial cells. Brackets, injury site. Scale bar, 100 μm (A, C).

(B) Quantification of CM proliferation in wt and *hsp70:dn-zrar* transgenic fish at 7 dpa. Data are mean ± SEM from 6 animals each (3097 wt and 2482 transgenic CMs analyzed). *$p < 3 \times 10^{-5}$, Student's t-test.

(C) Assessment of Mef2/PCNA double-positive cells (arrows) in wt and *hsp70:cyp26a1* transgenic fish at 7 dpa, after a single heat-shock at 6 dpa. Maximum projection images of 10 μm z-stacks are shown.

(D) Quantification of CM proliferation in wt and *hsp70:cyp26a1* transgenic fish at 7 dpa. Data are mean ± SEM from 4 wt and 6 transgenic animals (3888 wt and 4760 transgenic CMs analyzed). *$p < 2 \times 10^{-4}$, Student's t-test.

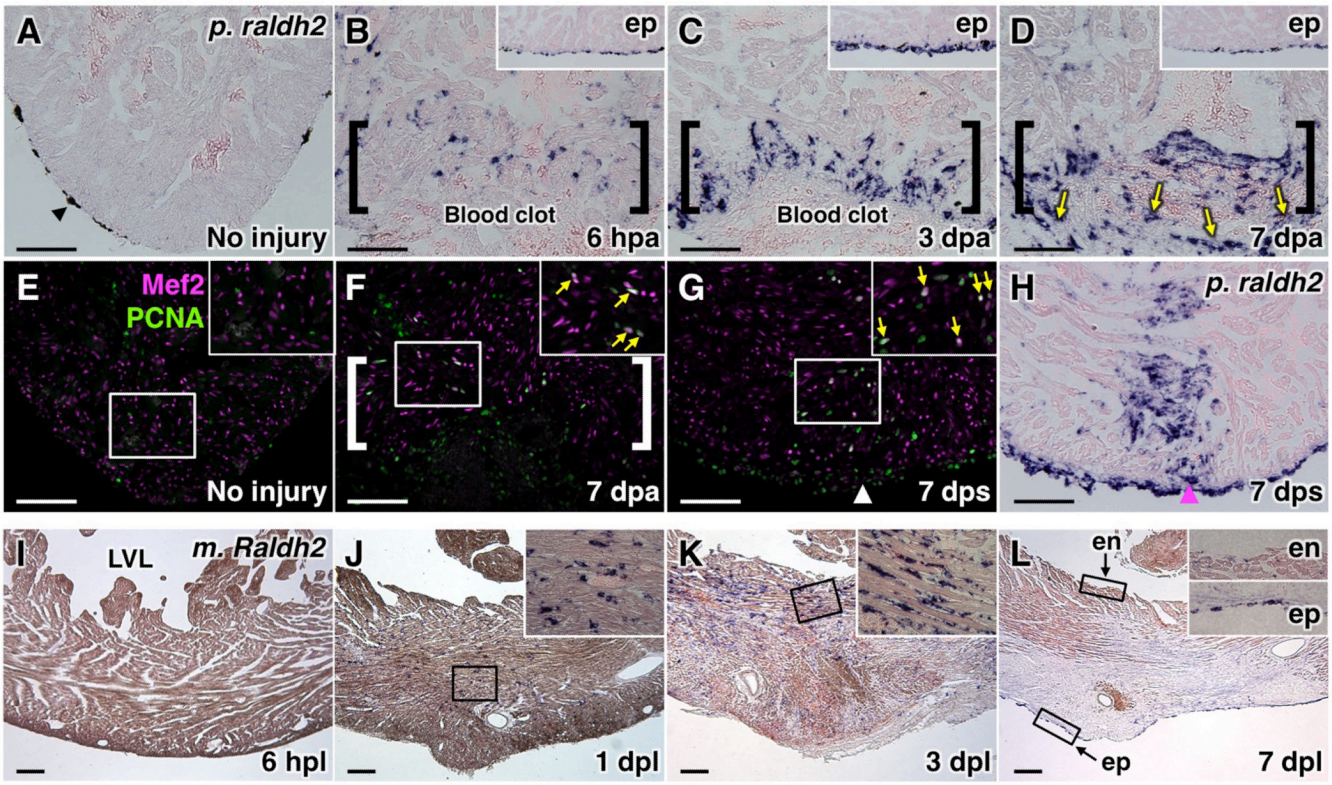

M

Injury responses:	*Polypterus senegalus*	*Danio rerio*	*Mus musculus*
Organ-wide epicardial *raldh2* expression	++	++	–
Organ-wide endocardial *raldh2* expression	+	++	–
Sustained epicardial *raldh2* in injuries	++	++	+
Sustained endocardial *raldh2* in injuries	++	++	–
Cardiomyocyte regeneration	+	++	–

Figure 4. Cardiac Injury Responses in Polypterus, Mouse, and Zebrafish

(A–D) *raldh2* (*p. raldh2*) expression by *in situ* hybridization in uninjured (A) and injured (B–D) polypterus ventricles. Arrowheads in (A), pigment cells. Brackets in (B–D), injury site. Insets in (B–D), lateral ventricular wall including epicardium (ep). Arrows in (D), *p. raldh2*-expressing epicardial cells. Scale bar, 100 μm (A–H).

(E–G) Assessment of $Mef2^{+}PCNA^{+}$ cells (arrows) in uninjured (E) and injured (F, G) polpyterus ventricles. Brackets in (F), injury site. Insets, high-zoom images of the rectangle. Arrowhead in (G), entry site of glass needle. Arrows in (F, G), proliferating CMs.

(H) *In situ* hybridization of *p. raldh2* after stab injury (arrowhead).

(I–L) *Raldh2* (*m. Raldh2*) expression by *in situ* hybridization at various timepoints post-ligation (pl). Insets in (J–L), high-zoom images of the rectangle. LVL, left ventricular lumen; ep, epicardium; en, endocardium. Scale bar, 200 μm.
(M) Summary of injury responses observed in polypterus, zebrafish, and mouse hearts.